Supporting Information for

# Ternary MOFs-Based Redox Active Sites Enabled 3D-on-2D Nanoarchitectured Battery-Type Electrodes for High-Energy Density Supercapatteries

Goli Nagaraju[1, 2], S. Chandra Sekhar[1], Bhimanaboina Ramulu[1], Sk. Khaja Hussain[1, 2], D. Narsimulu[1], Jae Su Yu[1, *]

[1]Institute for Wearable Convergence Electonics, Department of Electronic Engineering, Kyung Hee University, 1732 Deogyeong-daero, Yongin-si, Gyeonggi-do 17104, Republic of Korea

[2]Department of Chemical Engineering, College of Engineering, Kyung Hee University, 1732 Deogyeong-daero, Gihung-gu, Yongin-si, Gyeonggi-do 17104, Republic of Korea

*Corresponding author. E-mail: jsyu@khu.ac.kr (Jae Su Yu)

## Supplementary Figures and Tables

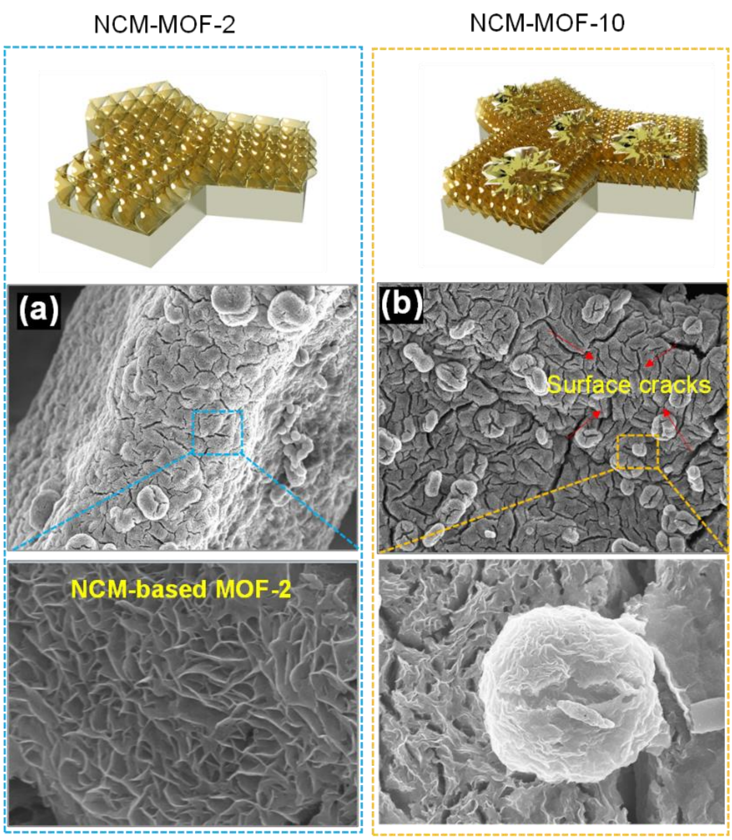


**Fig. S1** Low- and high-magnification SEM images of the (**a**) NCM-based MOF-2/Ni foam and (**b**) NCM-based MOF-10/Ni foam electrodes

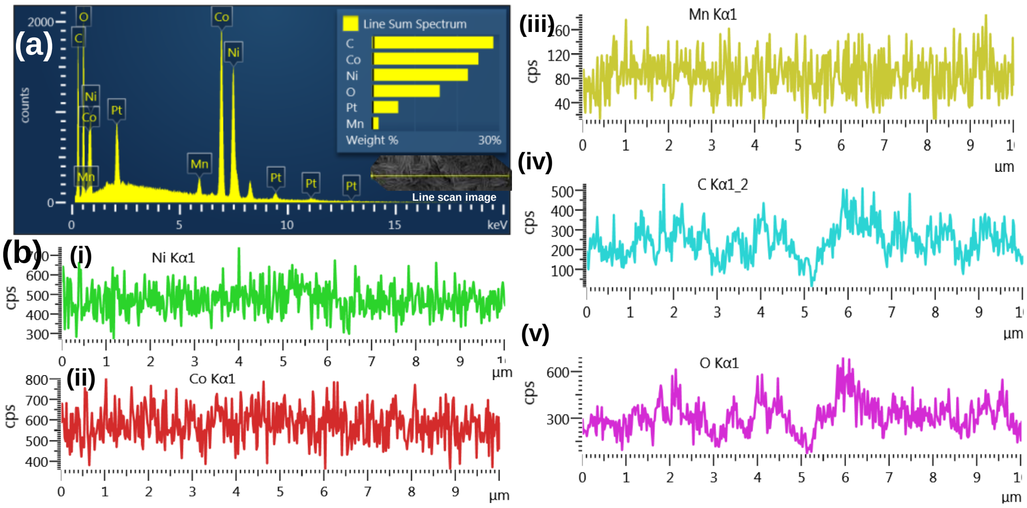

**Fig. S2** EDX spectrum and line-scan spectra of individual elements (Ni, Co, Mn, C and O) for the NCM-based MOF-5/Ni foam

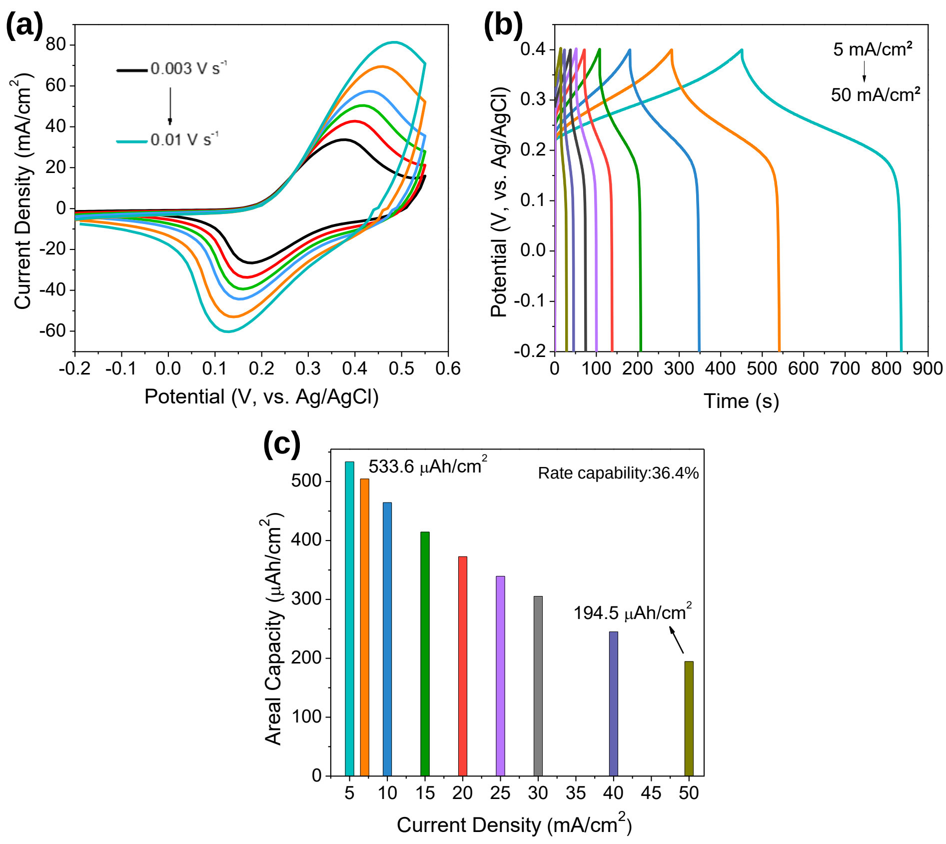


**Fig. S3** Electrochemical properties of the monolayered MOF-based NCM-2 tested in 1 M KOH electrolyte. (**a**) CV curves evaluated at different scan rates of 0.003-0.01 V $s^{-1}$, (**b**) GCD curves measured at different current densities of 5-10 mA $cm^{-2}$ and (**c**) estimated capacity values as a function of current density for the monolayered MOF-based NCM-2

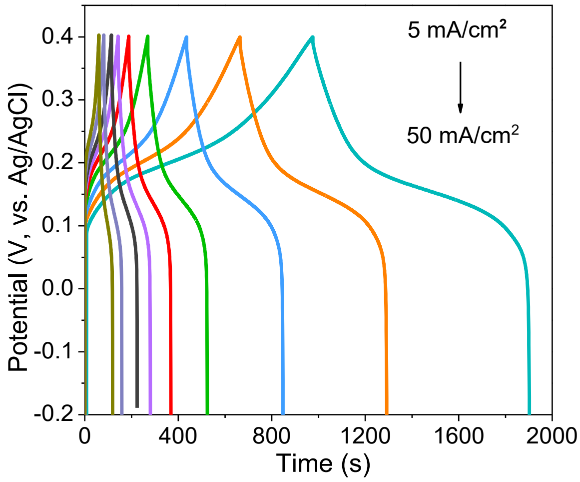


**Fig. S4** GCD curves measured at different current densities of 5-10 mA $cm^{-2}$ for the dual layered MOF-based NCM-5

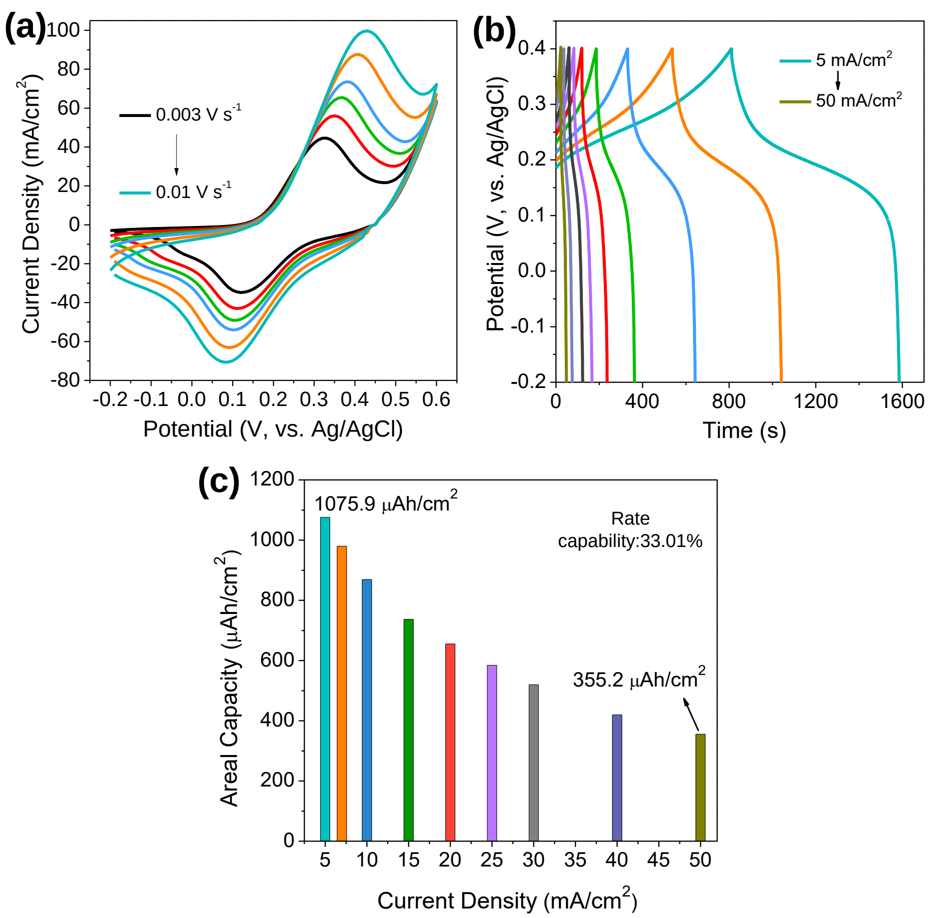


**Fig. S5** Electrochemical properties of the MOF-based NCM-10 evaluated in 1 M KOH electrolyte. (**a**) CV curves evaluated at different scan rates of 0.003-0.01 V $s^{-1}$, (**b**) GCD curves measured at different current densities of 5-10 mA $cm^{-2}$ and (**c**) caluclated capacity values with respect to the current densities of the MOF-based NCM-10

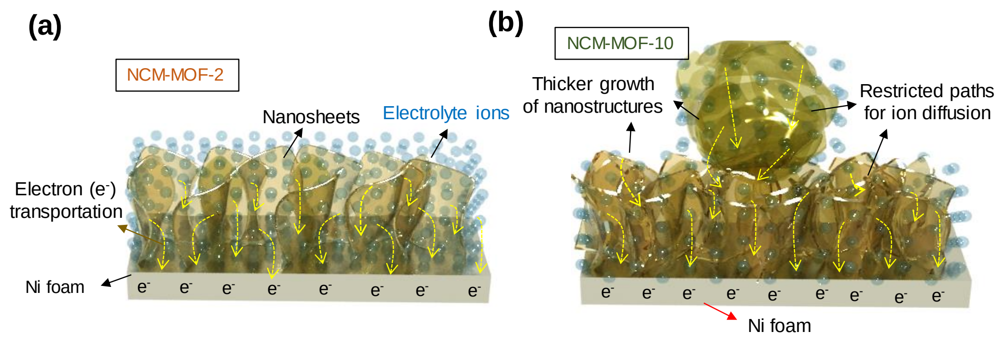


**Fig. S6** Schematic prediction of electrochemical merits/dissontvages of (**a**) NCM-based MOF-2 and (**b**) NCM-based MOF-10 electrodes during the energy storage process

**Table S1** Comparative energy storage performance of our dual layered NCM-based MOF with earlier reported metal oxide/sulfide and MOF-based materials in three-electrode system

| **Electroactive material** | **Morphology** | **Electrolyte** | **Test condition (mA cm$^{-2}$)** | **Area (cm$^2$)** | **Areal capacity (μAh cm$^{-2}$)** | **Refs.** |
|---|---|---|---|---|---|---|
| MOF-74 derived $Ni_xCo_{3-x}O_4$ | Nanoparticles | 6 M KOH | 6 | 1 | 325.83 | [S1] |
| Co-MOF | nanosheets | 5 M KOH | 4.5 | 1 | 1121.75 | [S2] |
| Co-MOF derived $Co_9S_8$@S,N-doped carbon materials | Cuboid structure | 6 M KOH | 2.4 | 1 | 143 | [S3] |
| Core–shell Ni-MOF-74@Co-MOF-74 derived $Ni_3S_4$@$Co_9S_8$ | Shell-in-shell tubes | 2 M NaOH | 2.4 | 1 | 367.47 | [S4] |
| Ni-MOF | Accordion-like nanosheets | 3 M KOH | 3.5 | 1 | 638.12 | [S5] |
| Ni-MOF/CNTs | Nanosheets | 6 M NaOH | 2 | 1 | 784.44 | [S6] |
| Ni-MOF | Sheet-like structure | 6 M KOH | 2.5 | 1 | 547.84 | [S7] |
| MOF-derived NiO | Porous nanoparticle | 6 M KOH | 5 | 1 | 201.25 | [S8] |
| MOF-derived NiO/ZnO | Hierarchical hollow spheres | 3 M KOH | 5.2 | 1 | 276.11 | [S9] |
| Zn/Co-ZIF derived Zn-Co-S | Rhombic dodecahedral cages | 6 M NaOH | 1 | 1 | 175.83 | [S10] |
| Ni-based MOF | Nanorods | 2 M KOH | 1.9 | 1 | 131.1 | [S11] |
| Bimetallic NiCo-MOF-74 | Spherical particles | 6 M KOH | 3 | 1 | 238.33 | [S12] |
| Ni-MOF derived NiO | Hexagonal flakes | 3 M KOH | 2 | 2 | 74.09 | [S13] |

| | | | | | | |
|---|---|---|---|---|---|---|
| MOF derived Ni–Co–S | Hierarchical nanosheets | 1 M KOH | 0.45 | 1 | 123.10 | [S14] |
| MOF-derived hollow porous $Ni_xP_yO_z$ | Microrods | 2 M KOH | 1.5 | 1 | 305.06 | [S15] |
| NCM-based MOF | Dual layered nanosheets/ nanoflowers | 1 M KOH | 5 | 1 | 1311.4 | This work |

**Table S2** Comparative areal energy and power density values of recently reported hybrid devices with our dual layered NCM-based MOF//AC supercapattery

| **Positive electrode material** | **Negative electrode material** | **Potential window** | **Areal $E_d$ (mWh $cm^{-2}$)** | **Areal $P_d$ (mW $cm^{-2}$)** | **Refs.** |
|---|---|---|---|---|---|
| Accordion-like Ni-MOF superstructure | Activated carbon | 1.2 V | 0.046 | 0.6 | [S5] |
| Ni-MOF/CNTs | rGO/g-$C_3N_4$ | 1.6 V | 0.1648 | 1.8 | [S6] |
| Onion-like nanoporous $CuCo_2O_4$ hollow spheres | Activated carbon | 1.5 V | 0.2437 | 3.75 | [S16] |
| MOF derived Ni–Co–S | Activated carbon | 1.7 V | 0.0955 | 3.27 | [S14] |
| MOF derived $MnO_x$–MHCF nanocubes | Activated carbon | 1.3 V | 0.0410 | 0.32 | [S17] |
| Hierarchical porous Ni-MOF | Activated carbon | 1.4 V | 0.0971 | 1.43 | [S18] |
| Ni-based MOF | Activated carbon | 1.2 V | 0.2 | 1.8 | [S19] |
| MOF derived Nanoporous $Co_3O_4$ | Nanoporous Carbon | 1.6 V | 0.0718 | 3.2 | [S20] |
| ZnO QDs/carbon/CNTs | N-doped carbon/CNTs | 1.7 V | 0.1030 | 3.69 | [S21] |
| Ni-Co MOF | Activated carbon | | 0.64 | 2.57 | [S22] |
| Co-Mn MOFs | Activated carbon | 1.6 | 0.12 | 4.68 | [S23] |
| Dual layered NCM-based MOFs | Activated carbon | 1.55 V | 1.21 | 5.3 | This work |


**Fig. S7** Powering multifunction electronic display by solar charge solitary supercapattery

## Supplementary References

[S1] S. Chen, M. Xue, Y. Li, Y. Pan, L. Zhu, S. Qiu, Rational design and synthesis of nixco3−xo4 nanoparticles derived from multivariate mof-74 for supercapacitors. J. Mater. Chem. A **3**(40), 20145-20152 (2015). https://doi.org/10.1039/C5TA02557E

[S2] J. Yang, Z. Ma, W. Gao, M. Wei, Layered structural Co-based MOF with conductive network frames as a new supercapacitor electrode. Chem. Eur. J. **23**(3), 631-636 (2017). https://doi.org/10.1002/chem.201604071

[S3] S. Liu, M. Tong, G. Liu, X. Zhang, Z. Wang et al., N-containing Co-MOF derived $Co_9S_8$@S,N-doped carbon materials as efficient oxygen electrocatalysts and supercapacitor electrode materials. Inorg. Chem. Front. **4**(3), 491-498 (2017). https://doi.org/10.1039/C6QI00403B

[S4] H. Li, F. Yue, H. Xie, C. Yang, Y. Zhang, L. Zhang, J. Wang, Hollow shell-in-shell $Ni_3S_4$@$Co_9S_8$ tubes derived from core–shell Ni-MOF-74@Co-MOF-74 as efficient faradaic electrodes. CrystEngComm **20**(7), 889-895 (2018). https://doi.org/10.1039/C7CE01873H

[S5] Y. Yan, P. Gu, S. Zheng, M. Zheng, H. Pang, H. Xue, Facile synthesis of an accordion-like Ni-MOF superstructure for high-performance flexible supercapacitors. J. Mater. Chem. A **4**(48), 19078-19085 (2016). https://doi.org/10.1039/C6TA08331E

[S6] P. Wen, P. Gong, J. Sun, J. Wang, S. Yang, Design and synthesis of Ni-MOF/CNT composites and RGO/carbon nitride composites for an asymmetric supercapacitor with high energy and power density. J. Mater. Chem. A **3**(26), 13874-13883 (2015). https://doi.org/10.1039/C5TA02461G

[S7] J. Yang, P. Xiong, C. Zheng, H. Qiu, M. Wei, Metal–organic frameworks: A new promising class of materials for a high performance supercapacitor electrode. J. Mater. Chem. A **2**(39), 16640-16644 (2014). https://doi.org/10.1039/C4TA04140B

[S8] Y. Han, S. Zhang, N. Shen, D. Li, X. Li, MOF-derived porous NiO nanoparticle architecture for high performance supercapacitors. Mater. Lett. **188**, 1-4 (2017). https://doi.org/10.1016/j.matlet.2016.09.051

[S9] G.-C. Li, P.-F. Liu, R. Liu, M. Liu, K. Tao et al., MOF-derived hierarchical double-shelled NiO/ZnO hollow spheres for high-performance supercapacitors. Dalton Trans. **45**(34), 13311-13316 (2016). https://doi.org/10.1039/C6DT01791F

[S10] P. Zhang, B.Y. Guan, L. Yu, X.W. Lou, Formation of double-shelled zinc–cobalt sulfide dodecahedral cages from bimetallic zeolitic imidazolate frameworks for hybrid supercapacitors. Angew. Chem. Int. Ed. **56**(25), 7141-7145 (2017). https://doi.org/10.1002/anie.201702649

[S11] C. Qu, Y. Jiao, B. Zhao, D. Chen, R. Zou, K.S. Walton, M. Liu, Nickel-based pillared MOFs for high-performance supercapacitors: Design, synthesis and stability study. Nano Energy **26**, 66-73 (2016). https://doi.org/10.1016/j.nanoen.2016.04.003

[S12] C. Young, J. Kim, Y.V. Kaneti, Y. Yamauchi, One-step synthetic strategy of hybrid materials from bimetallic metal–organic frameworks for supercapacitor applications. ACS Appl. Energy Mater. **1**(5), 2007-2015 (2018). https://doi.org/10.1021/acsaem.8b00103

[S13] S. Gao, Y. Sui, F. Wei, J. Qi, Q. Meng, Y. He, Facile synthesis of nickel metal–organic framework derived hexagonal flaky nio for supercapacitors. J. Mater. Sci. - Mater. Electron. **29**(3), 2477-2483 (2018). https://doi.org/10.1007/s10854-017-8169-7

[S14] K. Tao, X. Han, Q. Ma, L. Han, A metal–organic framework derived hierarchical nickel–cobalt sulfide nanosheet array on ni foam with enhanced electrochemical performance for supercapacitors. Dalton Trans. **47**(10), 3496-3502 (2018). https://doi.org/10.1039/C7DT04942K

[S15] R. Bendi, V. Kumar, V. Bhavanasi, K. Parida, P.S. Lee, Metal organic framework-derived metal phosphates as electrode materials for supercapacitors. Adv. Energy Mater. **6**(3), 1501833 (2016). https://doi.org/10.1002/aenm.201501833

[S16] A.A. Ensafi, S.E. Moosavifard, B. Rezaei, S.K. Kaverlavani, Engineering onion-like nanoporous $CuCo_2O_4$ hollow spheres derived from bimetal–organic frameworks for high-performance asymmetric supercapacitors. J. Mater. Chem. A **6**(22), 10497-10506 (2018). https://doi.org/10.1039/C8TA02819B

[S17] Y.-Z. Zhang, T. Cheng, Y. Wang, W.-Y. Lai, H. Pang, W. Huang, A simple approach to boost capacitance: Flexible supercapacitors based on manganese oxides@MOFs via chemically induced in situ self-transformation. Adv. Mater. **28**(26), 5242-5248 (2016). https://doi.org/10.1002/adma.201600319

[S18] P. Du, Y. Dong, C. Liu, W. Wei, D. Liu, P. Liu, Fabrication of hierarchical porous nickel based metal-organic framework (Ni-MOF) constructed with nanosheets as novel pseudo-capacitive material for asymmetric supercapacitor. J. Colloid Interface Sci. **518**, 57-68 (2018). https://doi.org/10.1016/j.jcis.2018.02.010

[S19] L. Kang, S.-X. Sun, L.-B. Kong, J.-W. Lang, Y.-C. Luo, Investigating metal-organic framework as a new pseudo-capacitive material for supercapacitors. Chin. Chem. Lett. **25**(6), 957-961 (2014). https://doi.org/10.1016/j.cclet.2014.05.032

[S20] R.R. Salunkhe, J. Tang, Y. Kamachi, T. Nakato, J.H. Kim, Y. Yamauchi, Asymmetric supercapacitors using 3d nanoporous carbon and cobalt oxide electrodes synthesized from a single metal–organic framework. ACS Nano **9**(6), 6288-6296 (2015). https://doi.org/10.1021/acsnano.5b01790

[S21] Y. Zhang, B. Lin, J. Wang, J. Tian, Y. Sun, X. Zhang, H. Yang, All-solid-state asymmetric supercapacitors based on ZnO quantum dots/carbon/CNT and porous n-doped carbon/CNT electrodes derived from a single ZIF-8/CNT template. J. Mater. Chem. A **4**(26), 10282-10293 (2016). https://doi.org/10.1039/C6TA03633C

[S22] Y. Wang, Y. Liu, H. Wang, W. Liu, Y. Li et al., Ultrathin NiCo-MOF nanosheets for high-performance supercapacitor electrodes. ACS Appl. Energy Mater. **2**(3), 2063-2071 (2019). https://doi.org/10.1021/acsaem.8b02128

[S23] S.H. Kazemi, B. Hosseinzadeh, H. Kazemi, M.A. Kiani, S. Hajati, Facile synthesis of mixed metal–organic frameworks: Electrode materials for supercapacitors with excellent areal capacitance and operational stability. ACS Appl. Mater. Interfaces **10**(27), 23063-23073 (2018). https://doi.org/10.1021/acsami.8b04502